Supporting Information

Reversible Generation of Labile Secondary Carbocations from Alcohols in the Nanospace of H-Mordenite and Their Long-lasting Preservation at Ambient Temperature

Yoichi Masui,[†,*] Taiki Hattori,[‡] and Makoto Onaka[†,*]

[†]Graduate School of Arts and Sciences, The University of Tokyo, 3-8-1 Komaba, Meguro-ku, Tokyo 153-8902

[‡]Graduate School of Science, The University of Tokyo, 7-3-1 Hongo, Bunkyo-ku, Tokyo 113-003

Table of Contents

1. Instrumentation and chemicals

NMR spectra were recorded by a Bruker Avance III 500 USPlus NMR spectrometer operated at 500 MHz for ^{1}H NMR and 126 MHz for ^{13}C NMR. The chemical shift values for ^{1}H and ^{13}C were referenced to Me_4Si and residual solvent resonances, respectively. Chemical shifts are reported in δ ppm. The coupling constants (*J*) are given in Hz. ^{13}C MAS NMR spectra were recorded on a Bruker Avance III 400 WB USPlus spectrometer operated at 100 MHz with a 4 mm zirconia rotor, at a spinning rate of 10 kHz and 25 °C. An external standard was used to calibrate the chemical shifts. UV-Vis adsorption spectra were obtained on a Jasco V-550 spectrometer with a 1 cm or 1 mm cell for the liquid samples or on a Jasco PSH-002 powder cell and ISV-469 integrating sphere equipment for the powder samples. Infrared spectra were measured on a Jasco FT / IR-6300 spectrophotometer using NaCl film. Thin-layer chromatography (TLC) was performed using commercially available 60 mesh silica gel plates visualized with short-wavelength UV light (254 nm). The powder forms of **H-Mor** (TOSOH Co., Ltd., HSZ-640HOA, Si/Al=9), **H-Y** (TOSOH Co., Ltd., HSZ-320HOA, Si/Al=2.75), **H-Beta** (TOSOH Co., Ltd., HSZ-940HOA, Si/Al=18.5), **H-ZSM-5** (Clariant Catalysts K.K., Si/Al=45), silica-alumina (JGC Catalysts and Chemicals, Ltd., JRC-SAH-1, Si/Al=1.85) were purchased and activated at 400 °C in a vacuum for 2 h.

The organic reagents were obtained from commercial suppliers or prepared according to standard procedures unless otherwise noted. All solvents were distilled prior to use.

2. Synthesis of starting materials

2a. Synthesis of ^{13}C-enriched 4,4'-difluorobenzhydrol (1')

Scheme S2a. Synthetic route for ^{13}C-enriched 4,4'-difluorobenzhydrol(**1'**)

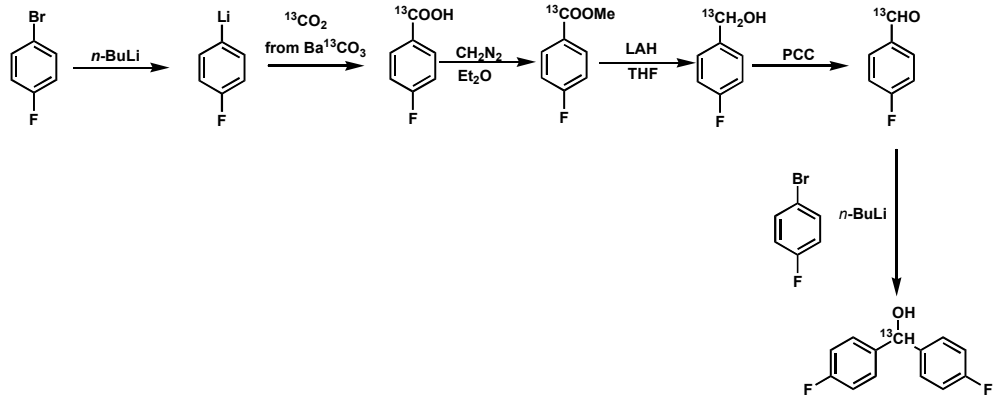

Synthesis of ^{13}C-enriched 4-fluorobenzoic acid

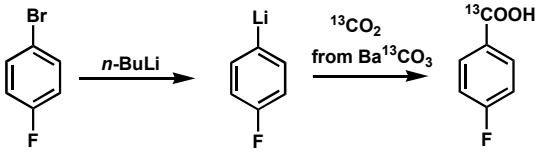

According to the known procedure,[S1] in a flame-dried 200-mL flask was placed 1-bromo-4-fluorobenzene (2.63 g, 1.65 mL, 15 mmol) and dry THF (50 ml) under nitrogen. To the solution was dropwise added *n*-BuLi (1.6 M in hexane, 9.1 mL, 15 mmol) over 20 min at -78 °C, and the mixture was stirred for 30 min and then cooled in a liquid nitrogen bath. Into the cooled mixture was introduced $^{13}CO_2$ gas that was produced by dropwise adding concentrated H_2SO_4 (25 mL, 480 mmol) to $Ba^{13}CO_3$ (2.7 g, 14 mmol) in another flame-dried 50 mL flask over 10 min. After stirred for an additional 10 min, the reaction mixture was slowly warmed to room temperature (rt) over 4 h. Fifty milliliters of H_2O was added to the reaction mixture, and the organic layer was separated. Twenty milliliters of 2 M HCl was added to the aqueous layer, and the aqueous layer was further extracted four times with 300 mL of Et_2O. The combined organic phase was dried over Na_2SO_4, and concentrated to afford the product (1.39 g, 10 mmol, 71% yield) as a white solid.

^{1}H NMR (500 MHz, $CDCl_3$): δ 8.15 – 8.13 (m, 4H), 7.26 – 7.15 (m, 4H). ^{13}C NMR (126 MHz, $CDCl_3$): δ 166.8 ($^{13}CO_2H$).

Synthesis of ^{13}C-enriched methyl 4-fluorobenzoate

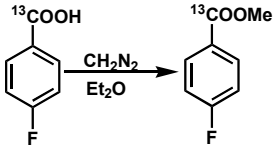

According to the procedure for the synthesis of diazomethane in the technical bulletin from Sigma-Aldrich, a mixture of H_2O (10 mL), EtOH (8 mL), and KOH (5.00 g, 89.3 mmol) was placed in the Aldrich Mini Diazald® apparatus, to which was dropwise added a solution of *N*-methyl-*N*-nitrosotoluene-4-sulphonamide (4.5 g, 21 mmol) in ether (50 mL) at 65 °C over 30 min. The formed diazomethane in Et_2O was introduced to a solution of ^{13}C-enriched 4-fluorobenzoic acid (1.4 g, 9,7 mmol) in Et_2O (30 mL) at rt. After the reaction mixture was stirred for 10 min, the remaining diazomethane was decomposed by adding acetic acid (1 M), and the organic layer was separated. The aqueous layer was further extracted four times with Et_2O (300 mL). The combined organic phase was dried over Na_2SO_4 and concentrated to afford the product (1.11 g, 7.2 mmol, 74% yield) as a colorless oil.

^{1}H NMR (500 MHz, $CDCl_3$): δ 8.07 – 8.05 (m, 4H), 7.12 – 7.09 (m, 4H), 3.93 (s, 3H). ^{13}C NMR (126 MHz, $CDCl_3$): δ 166.2 ($^{13}CO_2Me$), 132.1, 115.4, 115.3, 52.17.

Synthesis of ^{13}C-enriched 4-fluorobenzyl alcohol

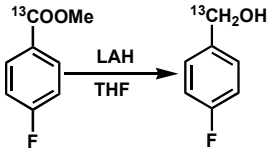

A solution of the ^{13}C-enriched methyl 4-fluorobenzoate (1.11 g, 7.2 mmol) in dry THF (10 mL) was added to the suspension of $LiAlH_4$ (0.60 g, 15.7 mmol) in dry THF (10 ml) at 0 °C over a period of 20 min, then the reaction mixture was stirred for 30 min at 0 °C. Fifty milliliters of a saturated aqueous solution of potassium sodium tartrate was added to the reaction mixture, and the organic layer was separated. The aqueous layer was further extracted four times with Et_2O (300 mL). The combined organic phase was dried over Na_2SO_4 and concentrated to afford the product (0.86 g, 6.8 mmol, 95% yield) as a colorless oil.

^{1}H NMR (500 MHz, $CDCl_3$): δ7.34 – 8.31 (m, 4H), 7.06 – 6.93 (m, 4H), 4.66 (dd, $J_{H\text{-}C}$ =

143 Hz, $J_{H\text{-}H}$ = 2.5 Hz, 3H). ^{13}C NMR (126 MHz, $CDCl_3$): δ 167.2, 157.4, 136.7, 136.6, 128.7, 128.6, 115.4, 115.3, 64.13 ($^{13}CH_2OH$).

Synthesis of ^{13}C-enriched 4-fluorobenzaldehyde

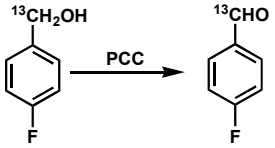

To a suspended mixture of ^{13}C-enriched 4-fluorobenzyl alcohol (0.86 g, 6.8 mmol) in dry CH_2Cl_2 (10 mL) and Celite (5.0 g) was added solid pyridinium chlorochromate (1.5 g, 6.9 mmol) at rt, and then the reaction mixture was stirred for 30 min at rt. After filtration and concentration of the reaction mixture, the organic residue was purified on a short silica gel column (hexane to CH_2Cl_2) to afford the product (0.80 g, 6.5 mmol, 59% yield) as a yellow oil.

^{1}H NMR (500 MHz, $CDCl_3$): δ 9.97 (d, $J_{H\text{-}C}$ = 172 Hz, 1H), 7.93 – 7.89 (m, 4H), 7.27 – 7.20 (m, 4H). ^{13}C NMR (126 MHz, $CDCl_3$): δ 190.5 (^{13}CHO), 171.6, 161.5, 132.4, 116.4, 116.2.

Synthesis of ^{13}C-enriched 4,4'-difluorobenzhydrol (1')

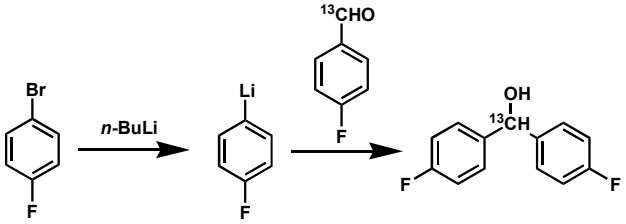

According to the known procedure,[S2] in a flame-dried 200 mL flask was placed 1-bromo-4-fluorobenzene (0.88 g, 0.55 mL, 5 mmol) and dry THF (50 mL) under nitrogen, and cooled to -78 °C, to which was then dropwise added *n*-BuLi (1.6 M in hexane, 3 mL, 5 mmol) over 20 min, and the mixture was stirred for 30 min. To the solution was dropwise added a solution of ^{13}C-enriched 4-fluorobenzaldehyde (0.50 g, 4.0 mmol) in dry THF (10 mL) over 20 min. After further stirred for 10 min, the reaction mixture was slowly warmed to rt over 4 h. Twenty milliliters of 2 M HCl was added, and the organic layer was separated. The aqueous layer was further extracted four times with Et_2O (300 mL). The combined organic phase was dried over Na_2SO_4 and concentrated to afford the crude product as a white solid, which was purified on a silica gel column (hexane to hexane/CH_2Cl_2 (1:1)) to afford the product (0.40 g, 1.8 mmol, 46% yield).

^{1}H NMR (500 MHz, $CDCl_3$): δ 7.32 – 7.25 (m, 4H), 7.04 – 7.00 (m, 4H), 5.81 (dd, $J_{H\text{-}C}$ = 144 Hz, $J_{H\text{-}H}$ = 3.3 Hz, 1H). ^{13}C NMR (126 MHz, $CDCl_3$): δ 163.2, 161.2, 139.4, 139.3, 128.2, 128.1, 115.4, 115.3, 74.92 (^{13}CHOH). FTIR (neat, NaCl): ν (O-H) 3370 cm^{-1}.

2b. Synthesis of ^{13}C-enriched 4,4'-difluorobenzophenone (5')

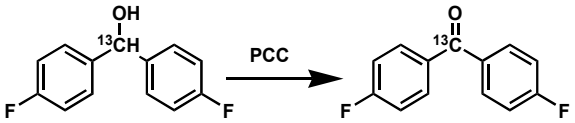

To a suspension of ^{13}C-enriched 4,4'-difluorobenzhydrol **1'** (0.44 g, 2.0 mmol) in dry CH_2Cl_2 (10 mL) and Celite (5.0 g) was added solid pyridinium chlorochromate (0.86 g, 4.0 mmol), and then the reaction mixture was stirred for 30 min at rt. After filtration and concentration of the reaction mixture, the organic residue was purified by short silica gel column chromatography (hexane to CH_2Cl_2) to afford the product (0.43 g, 2.0 mmol, 98% yield) as a white soild.

^{1}H NMR (500 MHz, $CDCl_3$): δ 7.83 – 7.80 (m, 4H), 7.19 – 7.16 (m, 4H). ^{13}C NMR (126 MHz, $CDCl_3$): δ 193.8 (^{13}C=O), 166.4, 164.4, 133.8, 133.7, 132.5, 115.6, 115.4. FTIR (neat, NaCl): ν (C=O) 1664 cm^{-1}.

2c. Synthesis of bis(1,1'-difluorodiphenylmethyl) ether (3)

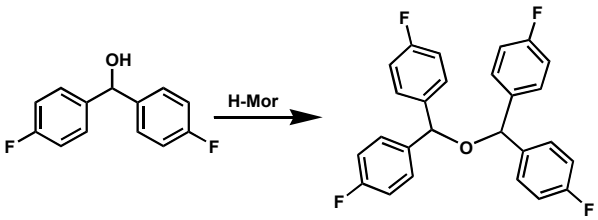

In a nitrogen atmosphere, 4,4'-difluorobenzhydrol **1** (0.2 g, 0.91 mmol) was added at rt to a CH_2Cl_2 (2 mL) suspension of **H-Mor** (200 mg), which had been activated in a vacuum at 400 °C for 2 h, and then the mixture wad stirred. The progress of the etherification reaction was monitored by silica gel thin layer chromatography. After the reaction was completed, the **H-Mor** was filtered off, and washed with CH_2Cl_2. Evaporation of the filtrate gave the crude product, which was further purified on a silica gel column (hexane to hexane/CH_2Cl_2 (4:1)) to afford the product (0.15 g, 0.36 mmol, 80% yield) as a white solid.

^{1}H NMR (500 MHz, $CDCl_3$): δ7.28 – 7.25 (m, 4H), 7.03 – 7.00 (m, 4H), 5.30 (s, 1H). ^{13}C NMR (126 MHz, $CDCl_3$): δ 163.2, 161.3, 137.4, 128.8, 128.7, 115.5, 115.4, 78.94.

3. Procedures for the UV-Vis measurement and results

3a. Typical procedure

Solid 4,4'-difluorobenzhydrol (**1**, 0.09 mmol) was mixed with powdery **H-Mor** (Si/Al = 9; 250 mg containing 0.42 mmol of aluminum), which was activated in a vacuum at 400 °C for 2 h, under a nitrogen atmosphere at rt. The mixture was stirred with a magnetic stir bar for 1 h with occasional vibration from a hand-held vibrator. The mixture was then placed on a diffuse reflectance cell in a glove bag filled with nitrogen gas, and subjected to UV-Vis measurements.

3b. Diffuse reflectance spectra of 1, benzhydrol, 4,4'-dichlorobenzhydrol, 9-fluorenol, and H-Mor

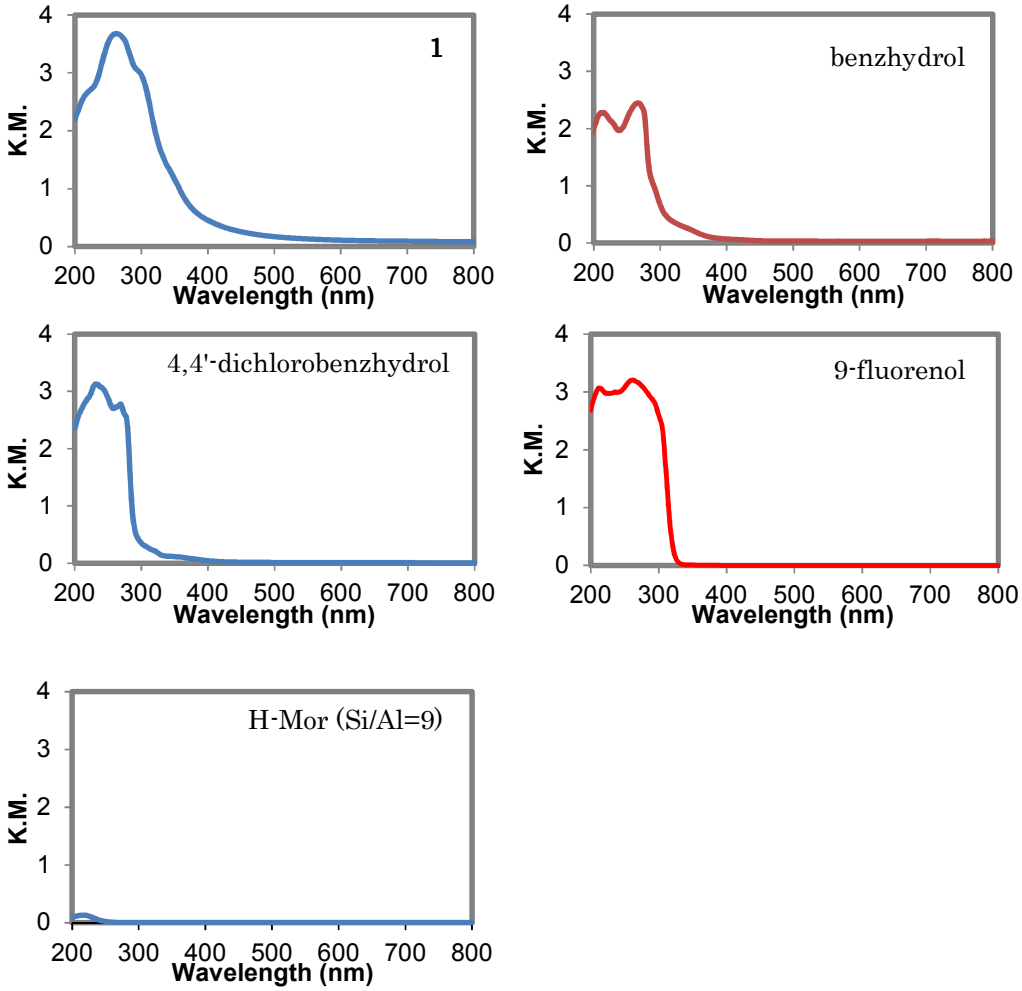

Figure S3b. Diffuse reflectance spectra of **1**, benzhydrol, 4,4'-dichlorobenzhydrol, 9-fluorenol, and **H-Mor**

4. Procedures for ^{13}C-MAS NMR measurement and results

4a. Typical procedure for the time course of ^{13}C-DD/MAS NMR spectra

Solid 4,4'-difluorobenzhydrol (**1'**, 0.09 mmol) was mixed with powdery **H-Mor** (Si/Al = 9; 250 mg containing 0.42 mmol of aluminum), which was activated in a vacuum at 400 °C for 2 h, under a nitrogen atmosphere at rt. The mixture was stirred with a magnetic stir bar for 1 h with occasional vibration from a hand-held vibrator. The mixture was then placed in a 4 mm zirconia rotor in a glove bag filled with nitrogen gas, and analyzed by ^{13}C-DD/MAS NMR with the parameters listed in Table S4a. The NMR measurement was run for 24 h.

Table S4a. Parameters for ^{13}C-DD/MAS NMR

Parameters	^{13}C-DD/MAS NMR
Accumulated time [h]	0.5
Dwell time [μs]	16.8
Relaxation delay [s]	10
^{13}C 90° pulse [μs]	3.4
^{13}C pulse length in decoupling sequence [μs]	4

4b. Time-dependent changes in solid state NMR spectra of the mixture of 1' and H-Mor

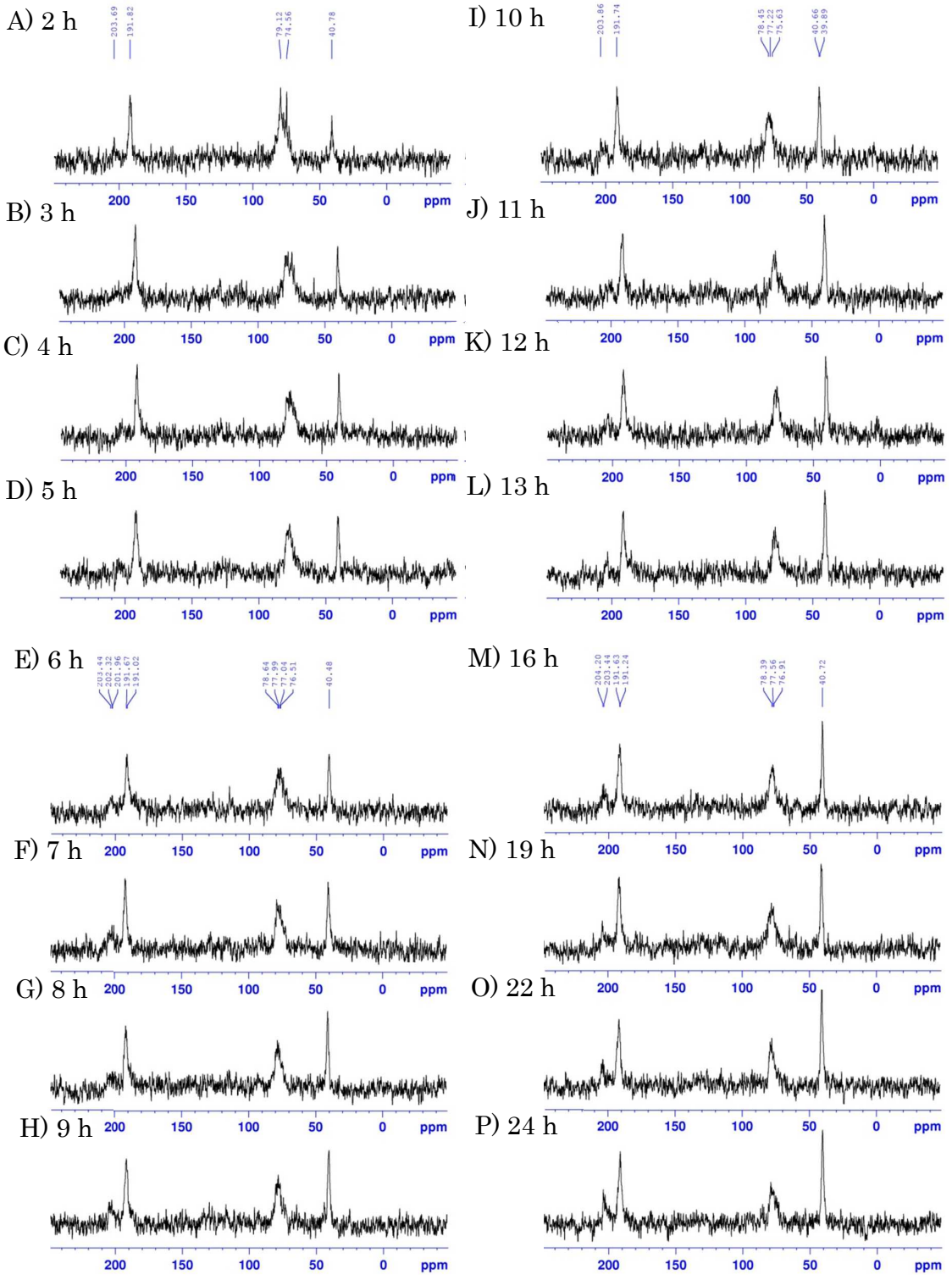

Figure S4a. Time-dependent changes in ^{13}C-DD/MAS NMR spectra of the mixture of 1'

and H-Mor

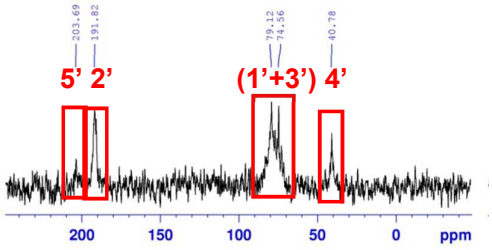

Peak areas of (**1'**+**3'**), **2'**, **4'**, and **5'**

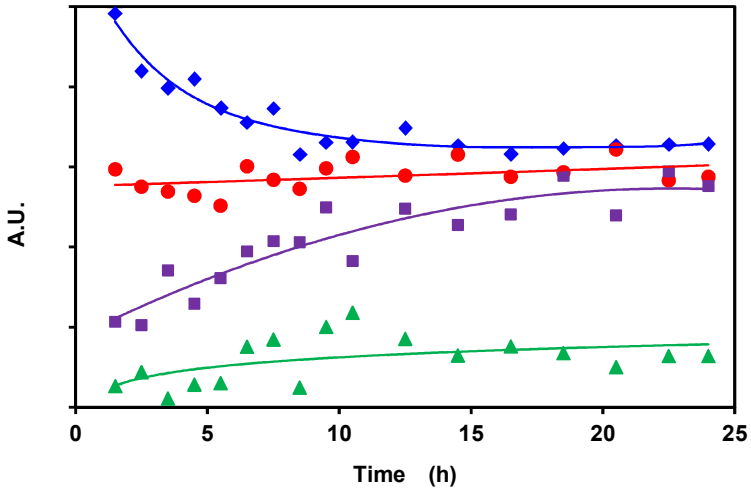

Figure S4b. Time-dependent changes in each peak area for (**1'**+**3'**) in blue, **2'** in red, **4'** in purple, and **5'** in green

From Figure S4a, it was found that the peak of **1'** at 74 ppm almost disappeared after 8 h. Figure S4b represents the time-dependent changes in the peak areas in the ^{13}C-DD/MAS NMR for (**1'**+**3'**) in which each peak partially overlapped and was difficult to be integrated apart, **4'**, and **5'** that were plotted every hour, showing that 1) the peak area of (**1'**+**3'**) gradually decreased and was constant after 8 h, 2) those of **4'** and **5'** gradually increased, and 3) that of **2'** remained almost constant.

4c. Typical procedure for the measurement of ^{13}C-CP/MAS NMR

Solid 4,4'-difluorobenzhydrol (**1'**, 0.09 mmol) was mixed with powdery **H-Mor** (Si/Al = 9; 250 mg containing 0.42 mmol of aluminum), which was activated in a vacuum at 400 °C for 2 h, under a nitrogen atmosphere at rt. The mixture was stirred with a magnetic stir bar for 1 h with occasional vibration from a hand-held vibrator. The mixture was then placed in a 4 mm zirconia rotor in a glove bag filled with nitrogen

gas, and analyzed by ^{13}C-CP/MAS NMR with the parameters listed in Table S4c.

Table S4c. Parameters for ^{13}C-CP/MAS NMR measurement

Parameters	^{13}C-CP/MAS NMR
Accumulated time [h]	12
Dwell time [μs]	16.8
Relaxation delay [s]	5
^{1}H channel for contact time [μs]	2000
^{13}C 90° pulse [μs]	3.4
^{13}C pulse length in decoupling sequence [μs]	6

4d. ^{13}C-CP/MAS NMR spectra of powder 1 and 3

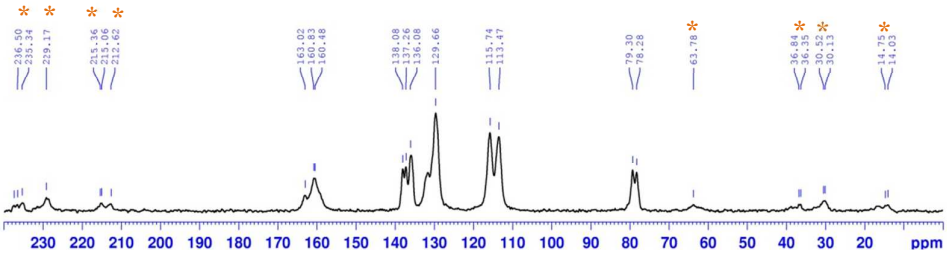

Figure S4c. ^{13}C-CP/MAS NMR spectrum of powder bis(4,4'-difluoropheylmethyl) ether (**3**); the asterisks show spinning side bands.

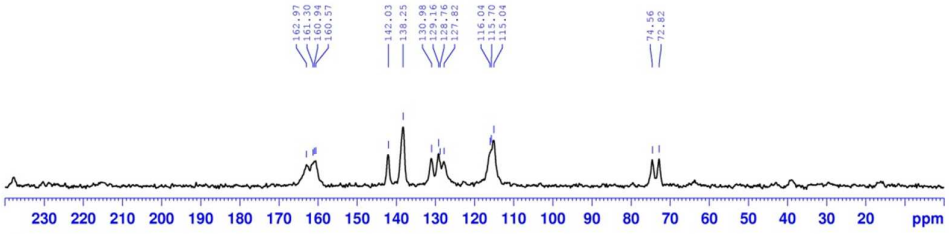

Figure S4d. ^{13}C-CP/MAS NMR spectrum of powder 4,4'-difluorobenzhydrol (**1**)

4e. Typical procedure for the measurement of ^{13}C-DD/MAS NMR

Solid 4,4'-difluorobenzhydrol (**1'**, 0.09 mmol) was mixed with powdery **H-Mor** (Si/Al = 9; 250 mg containing 0.42 mmol of aluminum), which was activated in a vacuum at 400 °C for 2 h, under a nitrogen atmosphere at rt. The mixture was stirred with a magnetic stir bar for 1 h with occasional vibration from a hand-held vibrator. The mixture was then placed in a 4 mm zirconia rotor in a glove bag filled with nitrogen gas, and analyzed by ^{13}C-DD/MAS NMR using the depth pulse program with the parameters listed in Table S4e.

Table S4e. Parameters for ^{13}C-DD/MAS NMR measurement

Parameters	^{13}C-DD/MAS NMR
Accumulated time [h]	24
Dwell time [μs]	16.8
Relaxation delay [s]	10
^{13}C 90° pulse [μs]	3.4
^{13}C pulse length in decoupling sequence [μs]	4

4f. Typical procedure for ^{13}C-DD/MAS NMR of the samples that were exposed to moisture

After the ^{13}C-DD/MAS NMR measurement, the solid sample (250 mg) was removed from the rotor and placed on an evaporating dish. The sample on the dish was placed in a closed vessel containing a small amount of water in order to be exposed to moisture overnight. The moisturized sample was again measured by ^{13}C-DD/MAS NMR with the parameters listed in Table S4e.

4g. The NMR spectrum of the mixture of 5' and H-Mor

Solid 4,4'-difluorobenzophenone (**5'**, 20 mg, 0.09 mmol) was mixed with powdery **H-Mor** (Si/Al = 9; 250 mg containing 0.42 mmol of aluminum**)**, which was activated in a vacuum at 400 °C for 2 h, under a nitrogen atmosphere at rt. The mixture was stirred with a magnetic stir bar for 1 h with occasional vibration from a hand-held vibrator. The mixture was then placed in a zirconia NMR rotor in a glove bag filled with nitrogen gas, and measured by ^{13}C-DD/MAS NMR with the parameters listed in Table S4e.

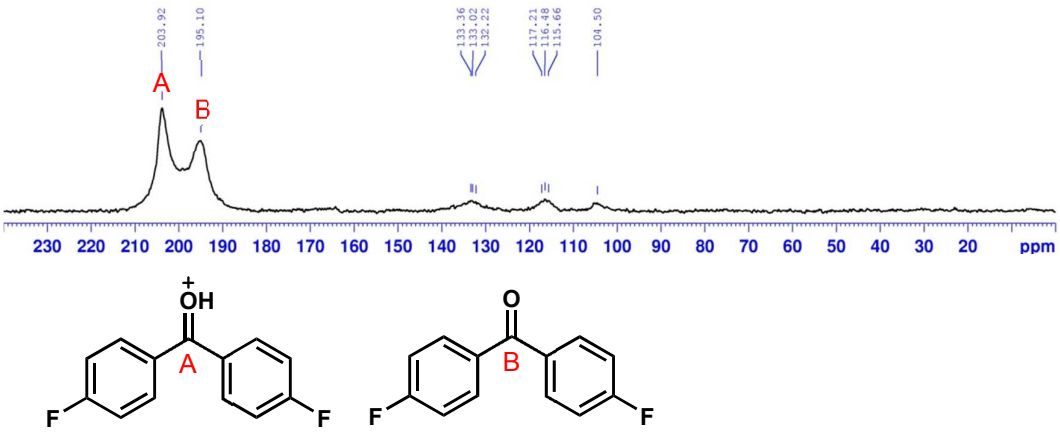

Figure S4e. ^{13}C-DD/MAS NMR spectrum of the mixture of **5'** and **H-Mor**: Both carbonyl carbons of protonated **5'** (A) and neutral **5'** (B) were observed.

5. Procedures for the addition of MeOH to carbocations in zeolite from 1

5a. Procedures for the addition of MeOH to 2, followed by determination of the products

Solid 4,4'-difluorobenzhydrol (**1**, 0.45 mmol) was mixed with powdery **H-Mor** (Si/Al = 9; 1.5 g containing 2.52 mmol of aluminum), which was activated in a vacuum at 400 °C for 2 h, under a nitrogen atmosphere at rt. The mixture was stirred with a magnetic stirr bar for 1 or 12 h with occasional vibration from a hand-held vibrator. Dry MeOH (30 mL) was then added to the mixture, and the mixture was stirred under a nitrogen atmosphere at rt overnight. **H-Mor** was filtered off with filter paper and washed with CH_2Cl_2. The combined organic layers were concentrated to afford a mixture of products, which were dissolved in $CDCl_3$ and analyzed by ^{1}H NMR.

TfOH (0.13 mmol) in $CDCl_3$ (0.48 mL) was slowly added to **1** (0.05 mmol) at rt. After stirring for 1 or 12 h at rt, the mixture was dissolved in $CDCl_3$, and analyzed by ^{1}H

NMR.

5b. Spectra for the products in the above reaction of 5a

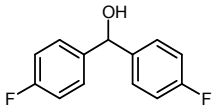

^{1}H NMR (500 MHz, $CDCl_3$) δ 7.25 – 7.32 (m, 4H), 7.00 – 7.04 (m, 4H), 5.74 (d, J = 4 Hz, 1H). ^{13}C NMR (126 MHz, $CDCl_3$) δ 163.2, 161.2, 139.4, 128.2, 115.4, 115.3, 74.92. FTIR (neat, NaCl): ν (O-H) 3370 cm^{-1}.

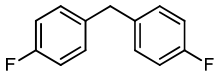

^{1}H NMR (500 MHz, $CDCl_3$) δ7.08 – 7.09 (m, 4H), 6.95 – 6.97 (m, 4H), 3.89 (s, 2H). ^{13}C NMR (126 MHz, $CDCl_3$) δ 162.4 160.5, 136.7, 136.6, 130.1, 115.3, 115.2, 40.15.

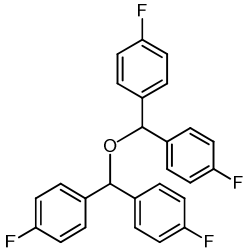

^{1}H NMR (500 MHz, $CDCl_3$) δ7.25 – 7.28 (m, 4H), 7.00 – 7.03 (m, 4H), 5.30 (s, 1H). ^{13}C NMR (126 MHz, $CDCl_3$) δ 163.2, 161.3, 137.4, 128.8, 128.7, 115.5, 115.4, 78.94. FTIR (neat, NaCl): ν (C-O-C) 1063 cm^{-1}.

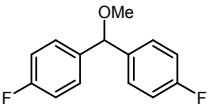

^{1}H NMR (500 MHz, $CDCl_3$) δ 3.35 (s, 3H) 5.20 (s, 1H), 7.00 – 7.03 (m, 4H), 7.25 – 7.29 (m, 4H), ^{13}C NMR (126 MHz, $CDCl_3$) δ 56.90, 83.96, 115.2, 115.4, 128.4, 128.5, 137.6, 137.7, 161.2, 163.1. FTIR (neat, NaCl): ν (C-O-C) 1100 cm^{-1}.

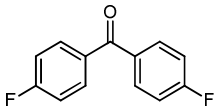

^{1}H NMR (500 MHz, $CDCl_3$) δ7.80 – 7.83 (m, 4H), 7.16 – 7.19 (m, 4H). ^{13}C NMR (126 MHz, $CDCl_3$) δ 193.8, 166.4, 164.4, 133.7, 132.5, 115.6, 115.4. FTIR (neat, NaCl): ν

(C=O) 1666 cm^{-1}.

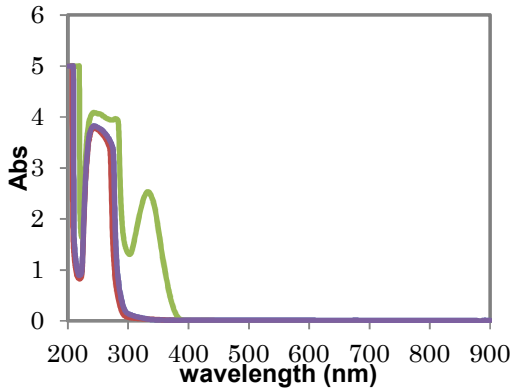

Figure S5a. UV-Vis spectra of products in CH_2Cl_2 solutions: **5** in green, **4** in purple, **6** in red, and **3** in blue (almost same figure to **4**)

5c. Procedures for the addition of MeOH to carbocations in zeolite from benzhydrol (1")

Solid benzhydrol (**1"**, 0.45 mmol) was mixed with powdery **H-Mor** (Si/Al = 9; 1.5 g containing 2.52 mmol of aluminum), which was activated in a vacuum at 400 °C for 2 h, in a nitrogen atmosphere at rt. The mixture was stirred with a magnetic stir bar for 12 h with occasional vibration from a hand-held vibrator. The dry MeOH (30 mL) was then added to the mixture, and the mixture was stirred overnight under a nitrogen atmosphere at rt. **H-Mor** was filtered off with filter paper and washed with CH_2Cl_2. The combined organic layers were concentrated to afford the mixture of products, which were dissolved in $CDCl_3$ and analyzed by ^{1}H NMR.

TfOH (0.13 mmol) in $CDCl_3$ (0.48 mL) was slowly added to **1"** (0.05 mmol) at rt. After stirred for 12 h (or 1 h in parentheses) at rt, the mixture was dissolved in $CDCl_3$, and analyzed by ^{1}H NMR and ^{1}H DOSY NMR.

5d. The yields of the products in the MeOH addition experiment

Table S5. The yields (%) of products **1"**-**6"** after the addition of MeOH to the mixture of **1"** and **H-Mor**.

Acid	**1"**	**6"**	**3"**	**4"**	**5"**	Total yield of **1", 3", 4", 5"**, and **6"**
H-Mor	54	5	19	0.1	1	78

5e. ^{1}H DOSY NMR spectra of the products from benzhydrol 1" upon contact with H-Mor or TfOH

(a)

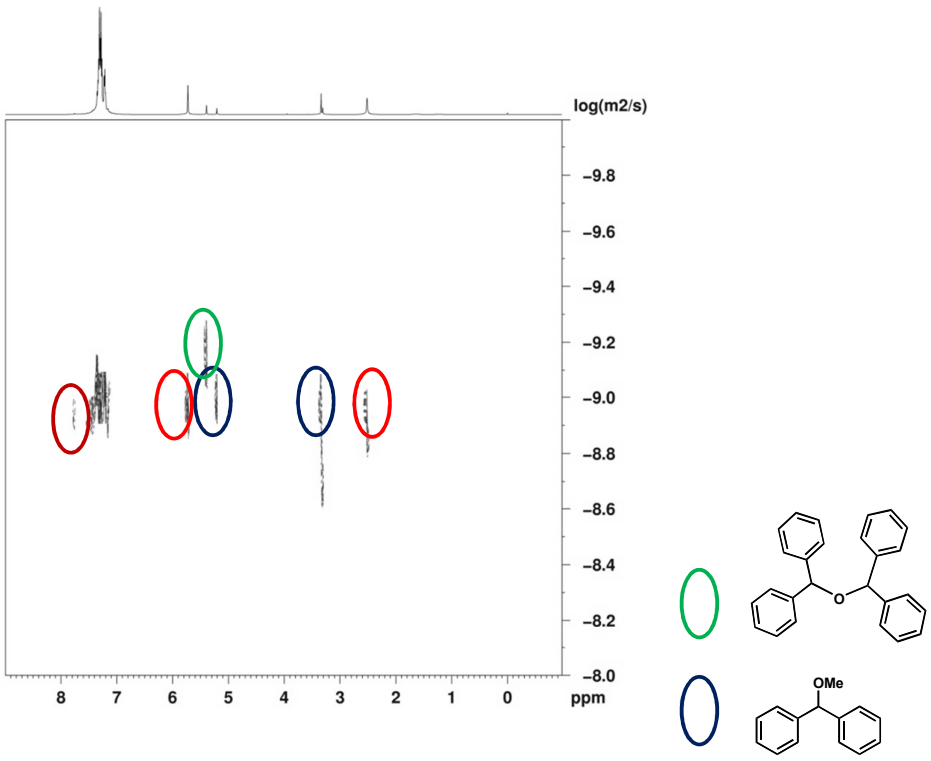

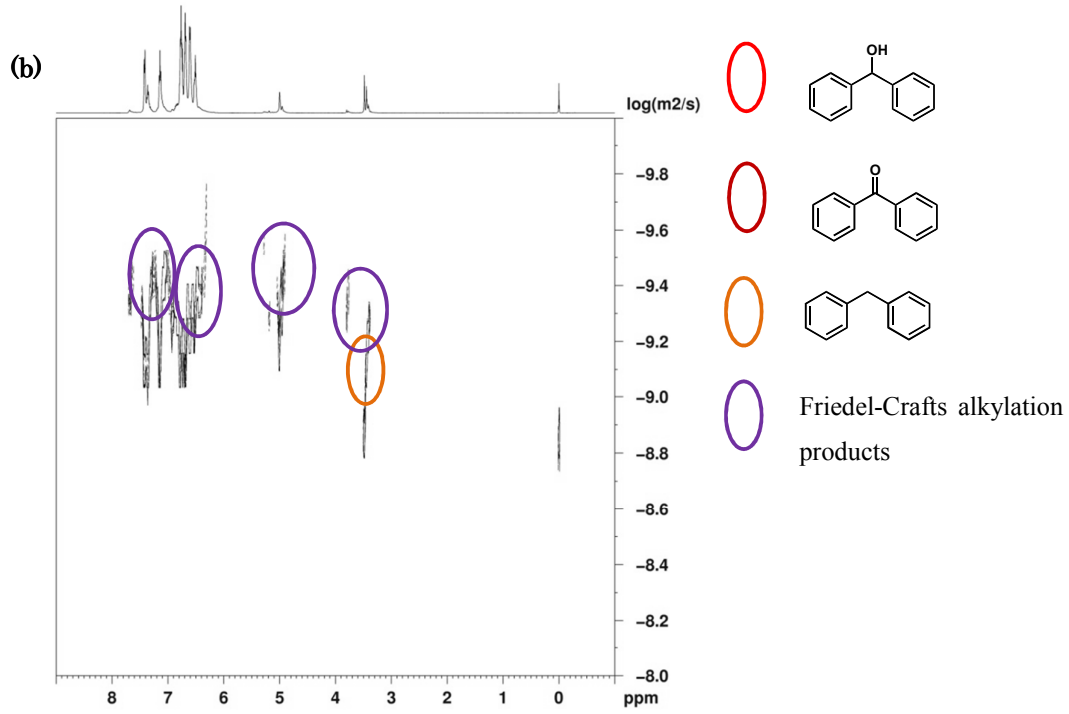

Figure S5b. ^{1}H DOSY spectra of the crude mixtures of benzhydrol **1"** with (a) **H-Mor** and (b) TfOH

6. Procedures and results for the generation of carbocation 2 from 3

Solid bis(4,4'-difluoropheylmethyl) ether **3** (9.8 mg, 0.05 mmol) was mixed with powdery **H-Mor** (Si/Al = 9; 250 mg containing 0.42 mmol of aluminum), which wa activated in a vacuum at 400 °C for 2 h, under a nitrogen atmosphere at rt. The mixture was stirred with a magnetic stirr bar for 1 h with occasional vibration from a hand-held vibrator. The mixture was then placed in a zirconia NMR rotor or a diffuse reflectance UV-Vis cell in a glove bag filled with nitrogen gas, and analyzed by ^{13}C-DD/MAS NMR with the parameters listed in Table S4e and UV-Vis spectroscopy.

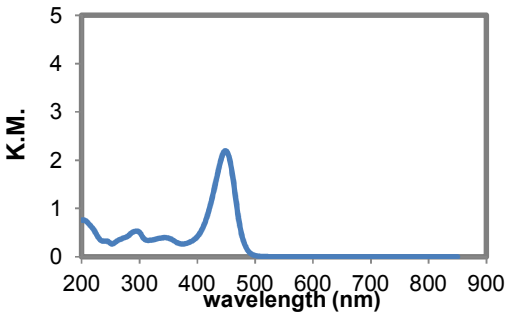

Figure S6a. UV-Vis spectrum after **3** was mixed with **H-Mor** for 1 h

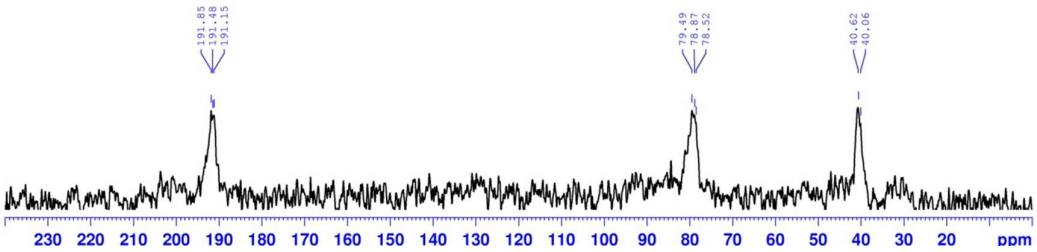

Figure S6b. ^{13}C-DD/MAS NMR after **3** was mixed with H-Mor for 1 h

Although the peak strength of **2** at 192 ppm from **3** was weaker than that from **1**, it was confirmed that **2** was similarly generated from **3** upon contact with **H-Mor**.

7. Stoichiometry between the number of starting material, acid sites, and generated molecules

Figure S7 shows the 120-T model (T = Si or Al sites) for a 4.4-nm long tubular pore of MOR zeolite main channel. H-Mor (Si/Al=9) is calculated to have 12 Al sites in the 120-T model, indicating there are twelve acid sites on the pore surface. Once three molecules of **1** are introduced in the pore and dehydrated, three cations of **2** as well as three H_3O^+ are formed, and six acid sites remain in the pore. Therefore, the number of acid sites on H-Mor we use turns out to be sufficient for the complete protonation to alcohol **1** under the present experimental conditions.

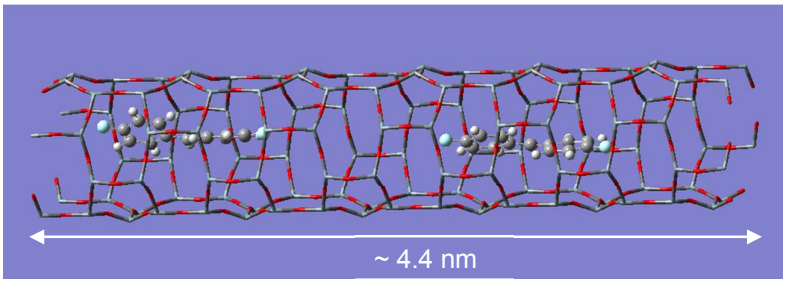

Figure S7. A 120-T model including two 4,4'-difluorodiphenylmethyl cations in a tubular pore of Mordenite zeolite.

We estimated the number of acid sites from the number of Al atom in order to simplify the discussion. According to the supplier's published data using NH_3 TPD measurement, **H-Mor** (Si/Al = 9) has 0.8 mmol/g of acid sites that can interact with NH_3 molecule. Because the number is about a half of that of Al site, we fixed the ratio of the number of the Al sites toward the number of the introduced alcohol **1** to be >4 as a precaution. Practically, the number of the acid sites should need less than 4 times that of alcohol **1** because one proton can trap more than one H_2O molecules in the side-pockets of the Mordenite pore system (See SI 8).

8. Dimensions of Mordenite pores as well as organic reactants and products which can intrude into the pores

Mordenite is composed of independent, one-dimensional straight main-channels with 12-membered ring openings of 0.70 x 0.65 nm in diameter, smaller 8-membered

sub-channels of 0.26 × 0.57 nm that lie parallel to the main-channels, and side-pockets with 8-membered rings of 0.34 × 0.48 nm that connect the 12-ring channel with the 8-ring channel through the 8-rings.[S3] Only the main-channels can be involved in accommodating large organic reactants and products in the present study (Figure S8a).

The main-channel of Mordenite has an ideal elliptical, columnar shape (Figure S8aB). Whether or not a molecule can enter the channel is determined by the dimensions of the *b* and *c* axes of a tri-axial ellipsoid simulating the molecule (Figure S8b, $a > b > c$)

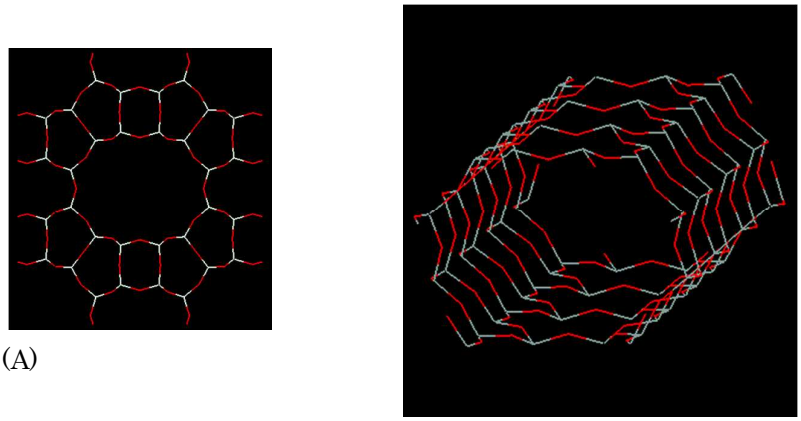

(A) (B)

Figure S8a. Images of Mordenite pores; (A) the cross section of the main and sub-channels , and (B) the three-dimensional shape of the main channel.

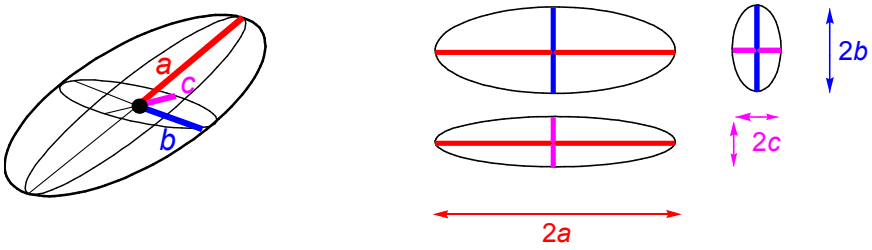

Figure S8b. Expression of a tri-axial ellipsoid ($a > b > c$).

9. Quantum chemical calculations for estimating the dissociating energies of alcohols to carbocations

We insisted "For the carbocations whose E values were defined by Mayr, a linear relationship between the calculated ΔE_{dis} values of the carbocations and experimental E values was found" in main text. A supplemental data of this is shown below.

All the energy values shown below were calculated at the B3LYP/6-31G(d) level using the Gaussian 03 program package.[S4] First, the thermodynamic stability of several carbocations was estimated by simple calculations of the dissociating energy of alcohols to carbocations and an OH- anion (ΔE_{dis}) (Figure 2). Then, we compared ΔE_{dis} to given Mayr's electrophilicity parameter E (Figure 1) for several carbocations that are strongly relevant to this study. As a result, the linear relationship of these two values were confirmed (Table S9, Figure S9a). Therefore, our attempt to estimate the stability of carbocations by simple calculation is reliable.

As an exception, the stability of a tropylium cation was underestimated due to the overestimate of the stability of cycloheptatrienyl alcohol in the gas phase calculation. Namely, cycloheptatrienyl alcohol was stabilized by the interaction between the π electrons and the hydroxyl proton. As witness, the C-O-H angle of cycloheptatrienyl alcohol was smaller than those of the other alcohols. On the other hand, for the experimental value in the solution, this interaction does not stand out due to the stabilization of –OH with solvents, and the dissociation energy should be estimated properly (Figure S9b).

Table S9. Mayr's E values and dissociation energy of an OH- anion from the corresponding alcohols (ΔE_{dis}) for the carbocations

	E [*a]	ΔE_{dis} (kcal/mol)
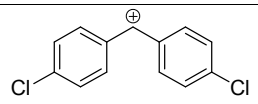	5.48	222.1
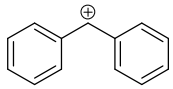	5.47	218.1
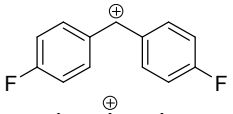	5.01	218.8
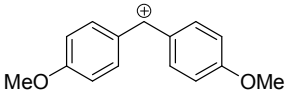	0	199.2

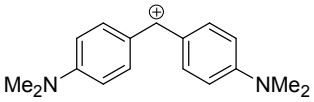	−7.02	181.2
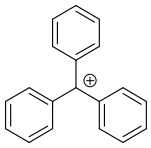	0.51	201.8
	−3.72	200.1

*a: Collectively summarized from refs 4(a) and 5(b).

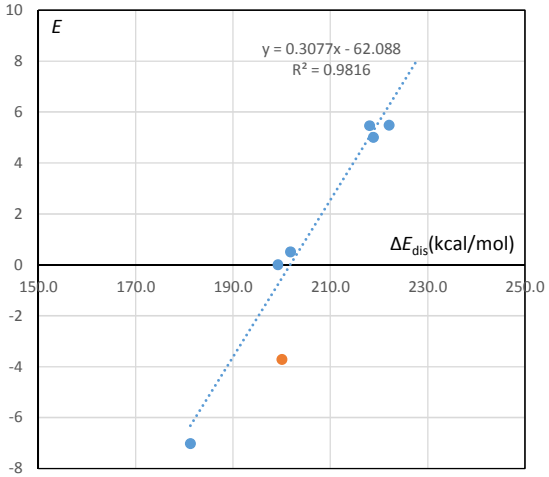

Figure S9a. The magnitude relationship between the ΔE_{dis} and the E values

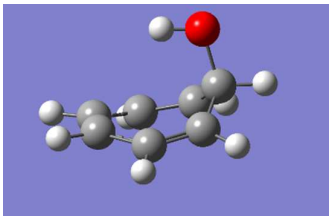

Figure S9b. The optimized structure of cycloheptatrienyl alcohol

10. Quantum chemical calculations of the activation energies of each side reaction

All the energy values shown below were calculated at the B3LYP/6-31G(d) level using the Gaussian 03 program package.[S4]

Alcohol **1** can intrude into the 12-membered main-channels of Mordenite to be protonated by the strongly acidic **H-Mor**, followed by dehydration to afford the carbocation **2** in the channel.

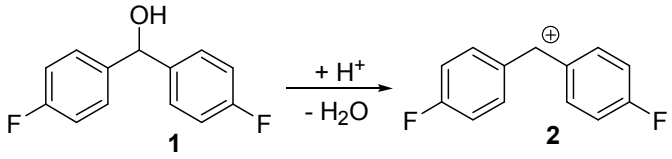

The etherification reaction of path **A** has a relatively smaller activation energy of 11.2 kcal/mol (Table S10a) and should be reversible. However, the reaction is unable to occur in the **H-Mor** pore because **3** is too large to be accommodated in the pore because the two benzene rings in each benzhydryl moiety are almost orthogonally oriented. So, it is difficult for any rotational conformer of **3** to fit in the pore with any rotation of any bonds in the molecule (Figure S10a(C)).

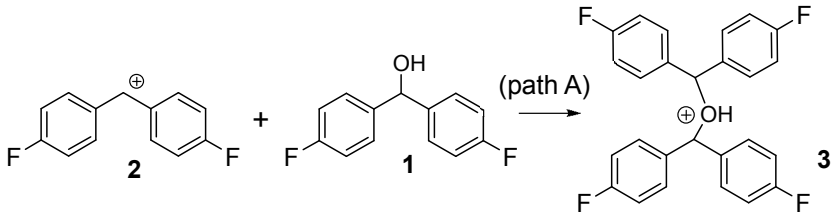

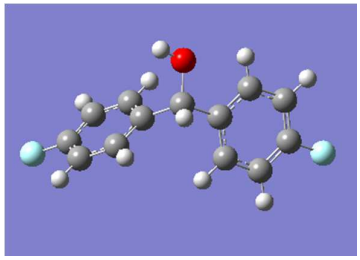

(A) **1** (2*a* = ~1.25 nm, 2*b* = ~0.58 nm, 2*c* = ~0.52 nm)

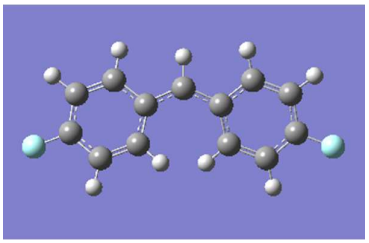

(B) **2** (2*a* = ~1.33 nm, 2*b* = ~0.54 nm, 2*c* = ~0.24 nm)

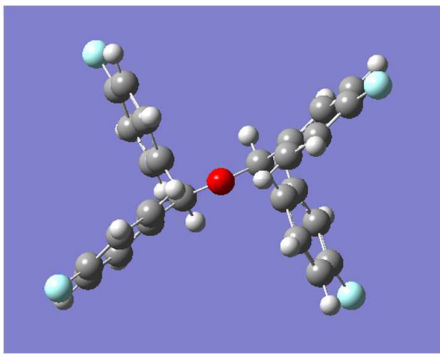

(C) **3** (2*a* = ~1.4 nm, 2*b* = ~1.2 nm, 2*c* = ~0.9 nm)

Figure S10a. The dimensions of (a) **1,** (b) **2,** and (c) **3**

Although both molecules **4** and **5**, can be accommodated in the channel of **H-Mor**, the size of the transition state for the reaction path **B** through a hydride transfer from the benzhydrol **1** to the cation **2** is larger than that of the Mordenite channel (Figure S10b(A)). Unlike the formation of ether **3**, the size of the transition state of the reaction path **B** can be reduced by adjusting the mutual orientation between **1** and **2**, but the reaction should be suppressed based on the relatively higher activation energy of 15.4 kcal/mol.

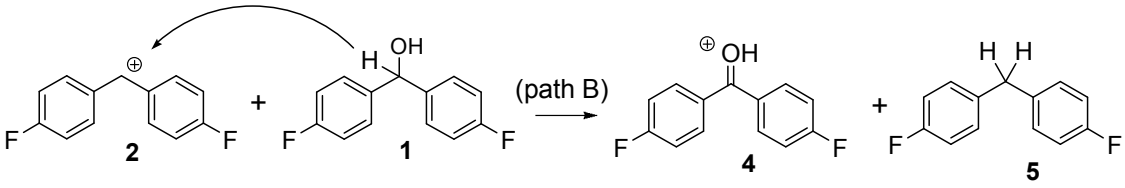

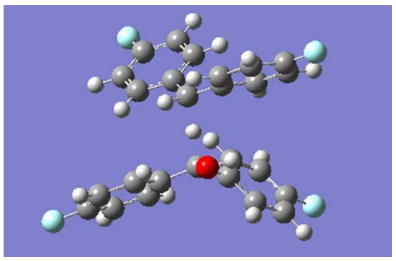

(A) ($2a$ = ~1.2 nm, $2b$ = ~0.9 nm, $2c$ = ~0.85 nm)

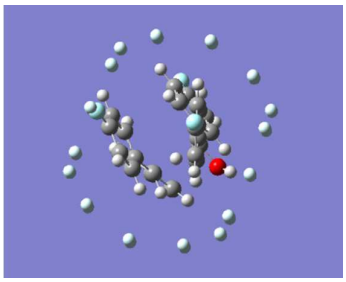

(B) ($2a$ = ~1.2 nm, $2b$ = ~0.68 nm, $2c$ = ~0.58 nm)

Figure S10b. The dimensions of the transition state of reaction path **B**; (A) the most stable transition state under free circumstances, and (B) a less stable transition state under confinement by the pore walls.

The Friedel-Crafts type reactions via path **C** cannot proceed for the 4,4'-difluorobenzhydrol due to the para-substituent on the benzene ring. For the non-substituted benzhydrol **1"**, the alkylation reaction cannot occur at least in the pores because the reaction path **C** has to go through a larger size transition state than the reaction path **B** (Figure S10c).

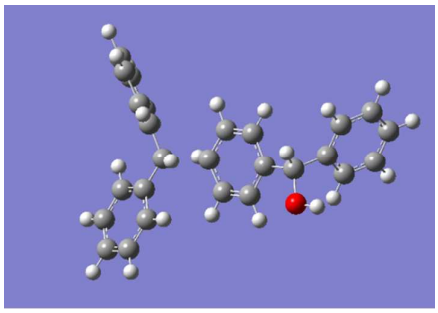

Figure S10c. The dimensions of the transition states of the reaction path **C** ($2a$ = ~1.41 nm, $2b$ = ~0.95 nm, $2c$ = ~0.52 nm).

Table S10a. Calculated activation energies for the side reactions via paths **A**, **B**, and **C**.

(kcal/mol)

		path **A**	path **B**	path **C**
benzhydorol (**1"**)	$\Delta E^{\ddagger}$	4.7	13.3	19.2
	$\Delta G^{\ddagger}$	**8.7**	**14.2**	**22.0**
4,4'-difluorobenzhydorol (**1**)	$\Delta E^{\ddagger}$	8.1	14.5	-
	$\Delta G^{\ddagger}$	11.2	15.4	-

11. References

S1) P, Woo.; Hartman, J.; Hayes, R. *J. Labelled Compd. Radiopharm.* **1999**, 42, 135-145.

S2) P, Mohan.; B, Akkattu.; G, Frank. *Org. Lett.*, **2011**, 13, 98–101.

S3) (a) Y, Komori.; S, Hayashi. P*hys. Chem. Chem. Phys.* **2003**, 5, 3777-3783. (b) Y, Komori.; S, Hayashi. *Bull. Chem. Soc. Jpn.* **2004,** 77, 673-679. (c) Huo, H.; Peng, L.; Gan, Z.; Grey, C. *J. Am. Chem. Soc.*, **2012**, 134, 9708–9720.

S4) Frisch, M. J.; Trucks, G. W.; Schlegel, H. B.; Scuseria, G. E.; Robb,M. A.; Cheeseman, J. R.; Montgomery, J. A., Jr.; Vreven, T.; Kudin, K. N.; Burant, J. C.; Millam, J. M.; Iyengar, S. S.; Tomasi, J.; Barone, V.; Mennucci, B.; Cossi, M.; Scalmani, G.; Rega, N.; Petersson, G. A.; Nakatsuji, H.; Hada, M.; Ehara, M.; Toyota, K.; Fukuda, R.; Hasegawa, J.; Ishida, M.; Nakajima, T.; Honda, Y.; Kitao, O.; Nakai, H.; Klene, M.; Li, X.; Knox, J. E.; Hratchian, H. P.; Cross, J. B.; Bakken, V.; Adamo, C.; Jaramillo, J.; Gomperts, R.; Stratmann, R. E.; Yazyev, O.; Austin, A. J.; Cammi,R.; Pomelli,C.;Ochterski, J.W.; Ayala, P.Y.;Morokuma, K.; Voth,G.A.; Salvador, P.; Dannenberg, J. J.; Zakrzewski,V.G.; Dapprich, S.; Daniels, A. D.; Strain, M. C.; Farkas, O.; Malick, D. K.; Rabuck,A.D.; Raghavachari,K.; Foresman, J. B.;Ortiz, J.V.; Cui,Q.; Baboul, A. G.; Clifford, S.; Cioslowski, J.; Stefanov, B. B.; Liu, G.; Liashenko, A.; Piskorz, P.; Komaromi, I.; Martin, R. L.; Fox,D. J.; Keith, T.; Al-Laham, M. A.; Peng, C. Y.; Nanayakkara, A.; Challacombe, M.; Gill, P. M.W.; Johnson, B.; Chen,W.;Wong, M. W.; Gonzalez, C.; Pople, J. A. Gaussian 03, revision D.01; Gaussian, Inc.: Wallingford, CT, 2004.

12. NMR spectra of reference compounds 1, 3, 4, 5, and 6

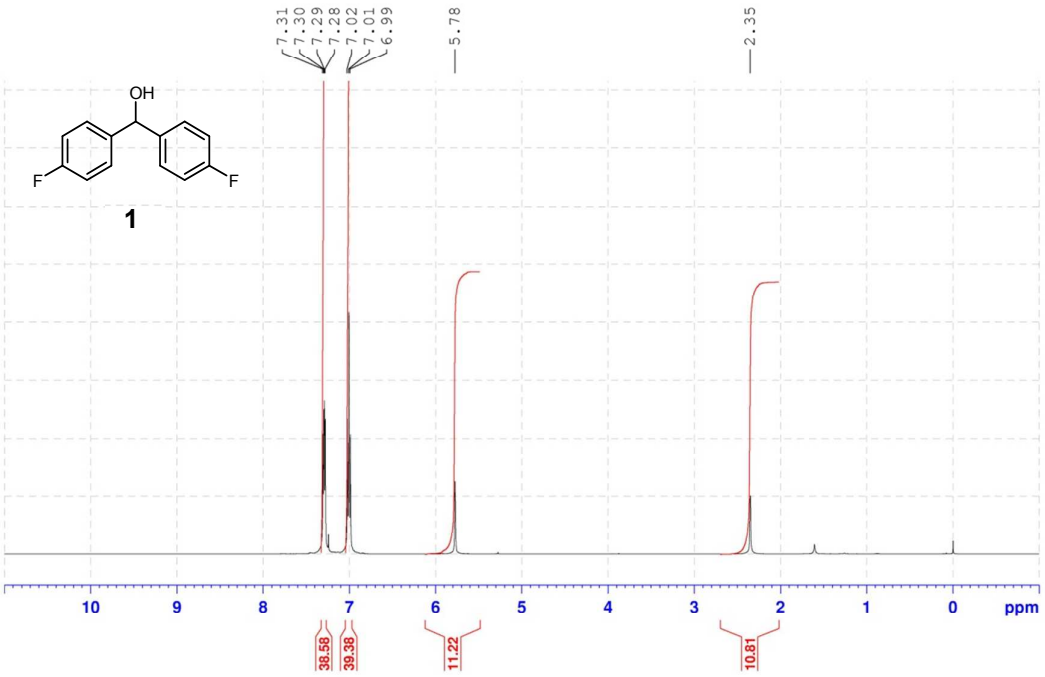

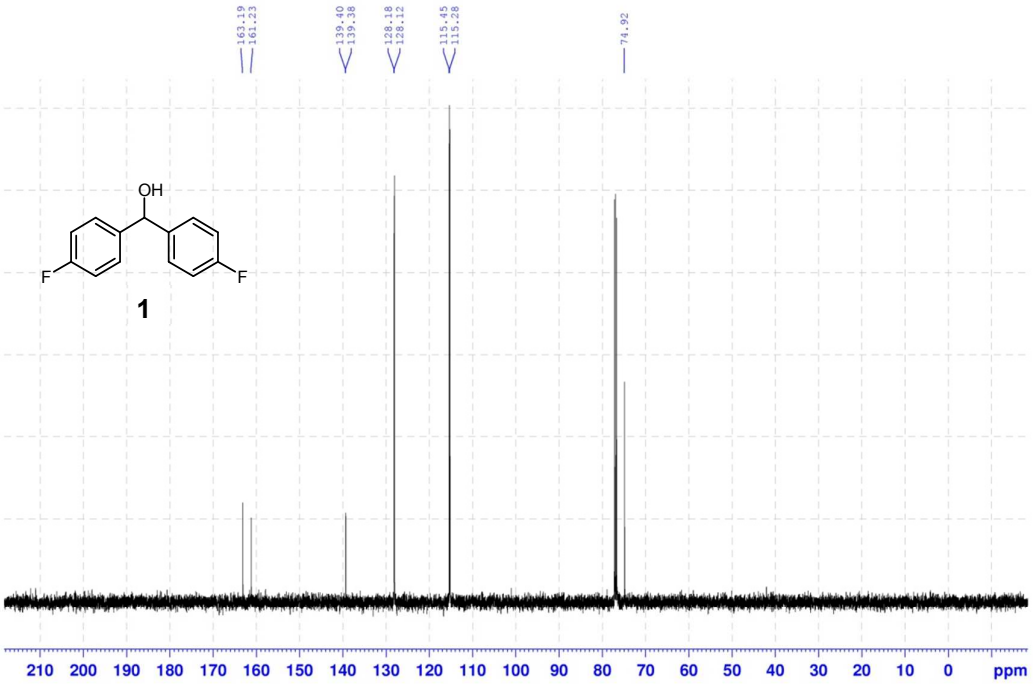

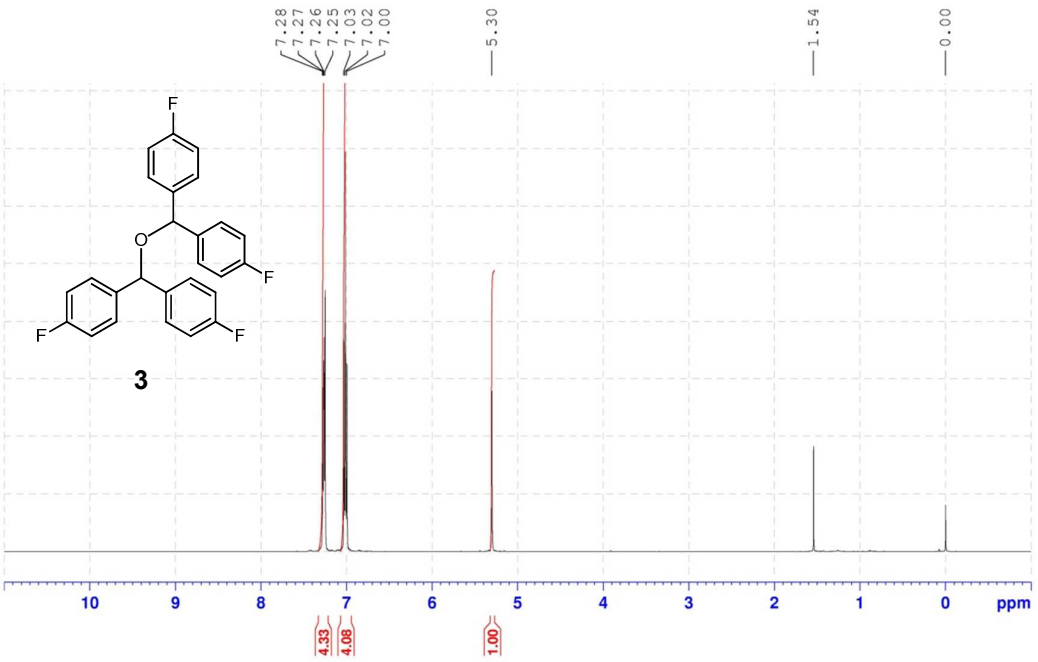
7.28
7.27
7.26
7.25
7.03
7.02
7.00
5.30
1.54
0.00
F
O
F
F
F
3
10
9
8
7
6
5
4
3
2
1
0
ppm
4.33
4.08
1.00

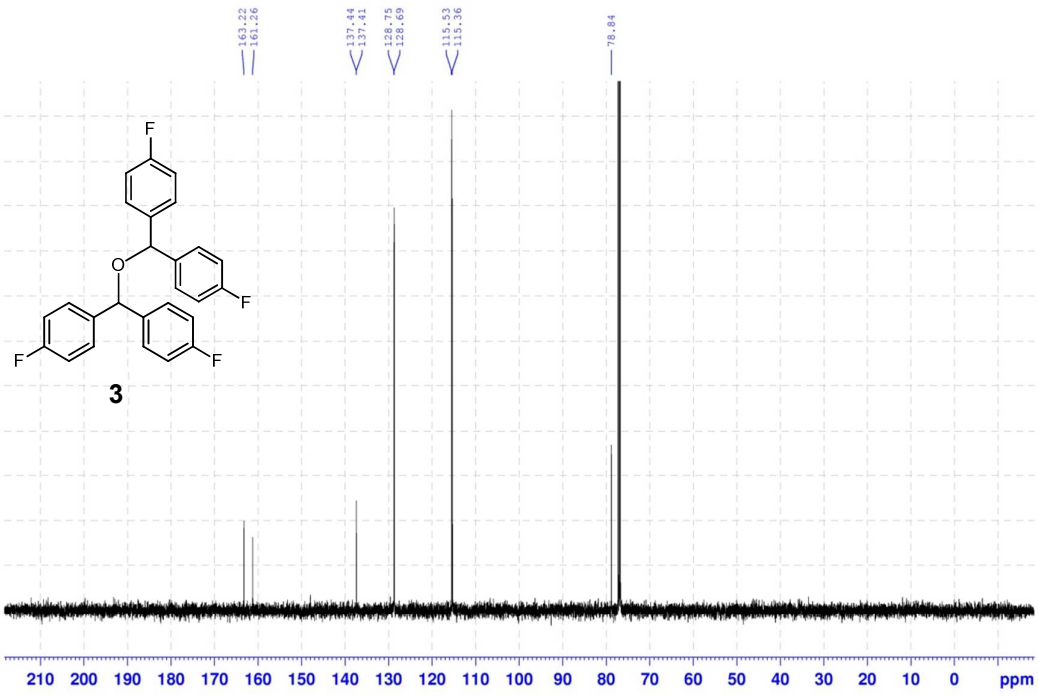
163.22
161.26
137.44
137.41
128.75
128.69
115.53
115.36
78.84
F
O
F
F
F
3
210
200
190
180
170
160
150
140
130
120
110
100
90
80
70
60
50
40
30
20
10
0
ppm

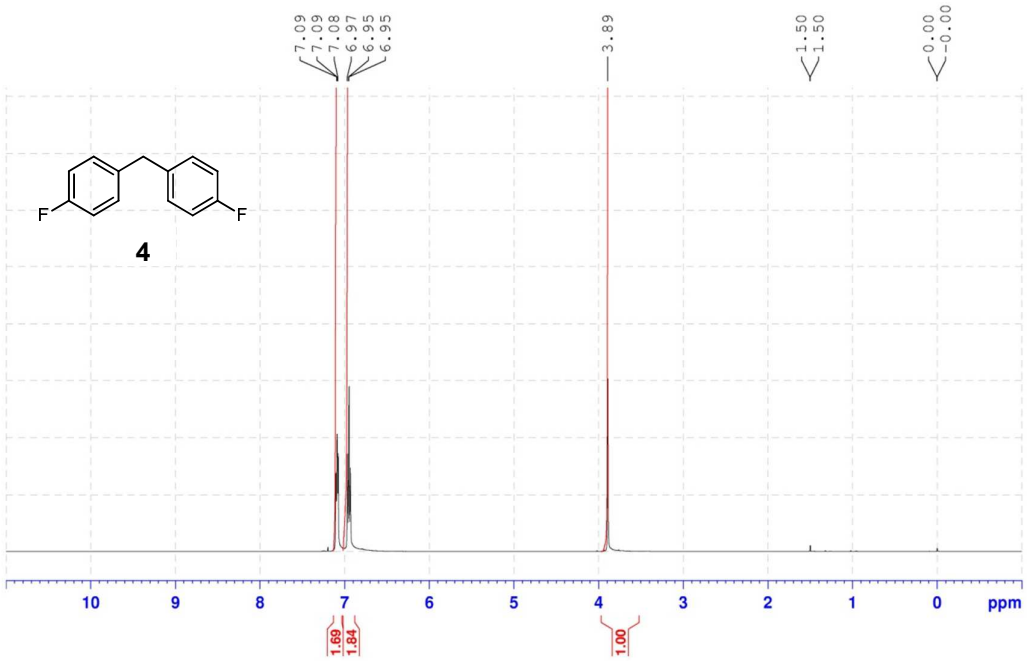
7.09
7.09
7.08
6.97
6.95
6.95
3.89
1.50
1.50
0.00
-0.00
F
F
4
10
9
8
7
6
5
4
3
2
1
0
ppm
1.69
1.84
1.00

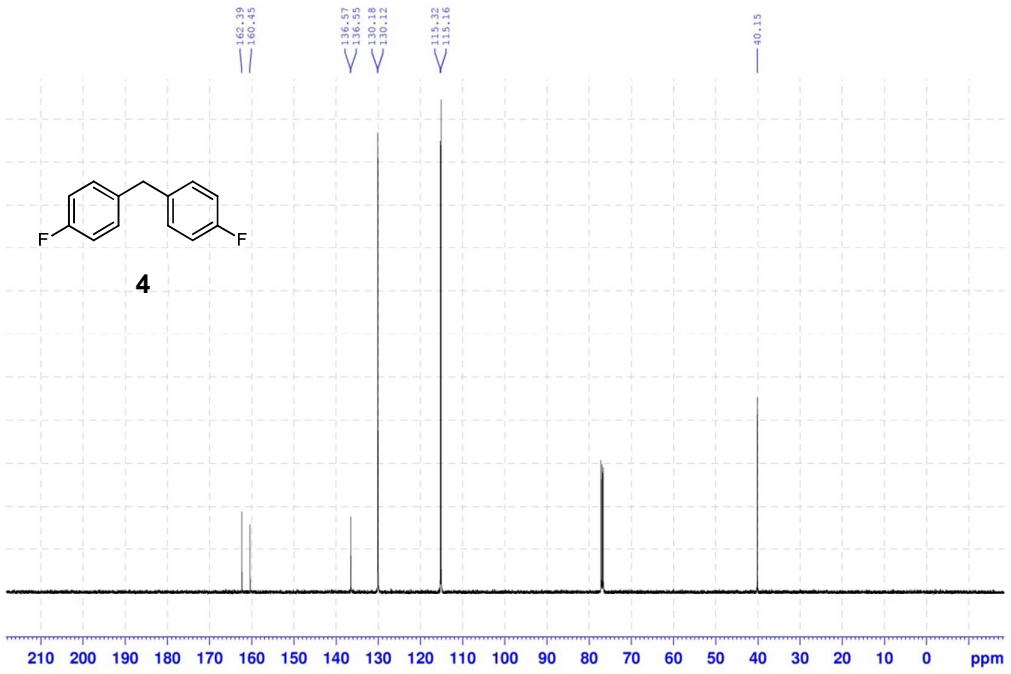
162.39
160.45
136.57
136.55
130.18
130.12
115.32
115.16
40.15
F
F
4
210
200
190
180
170
160
150
140
130
120
110
100
90
80
70
60
50
40
30
20
10
0
ppm

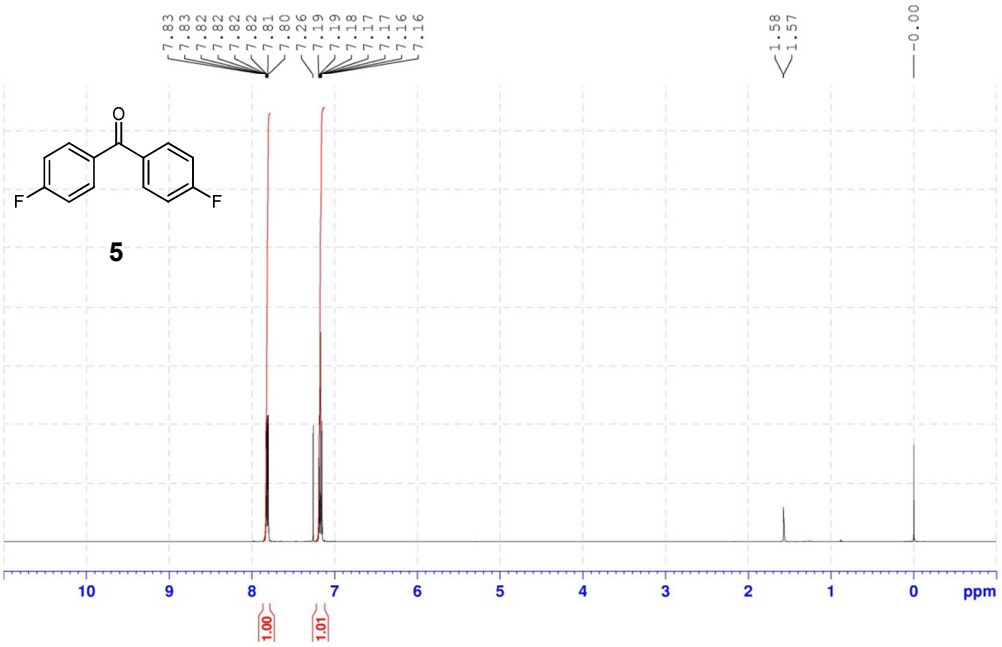
7.83
7.83
7.82
7.82
7.82
7.82
7.81
7.80
7.26
7.19
7.19
7.18
7.17
7.17
7.16
7.16
1.58
1.57
0.00
O
F
F
5
10
9
8
7
6
5
4
3
2
1
0
ppm
1.00
1.01

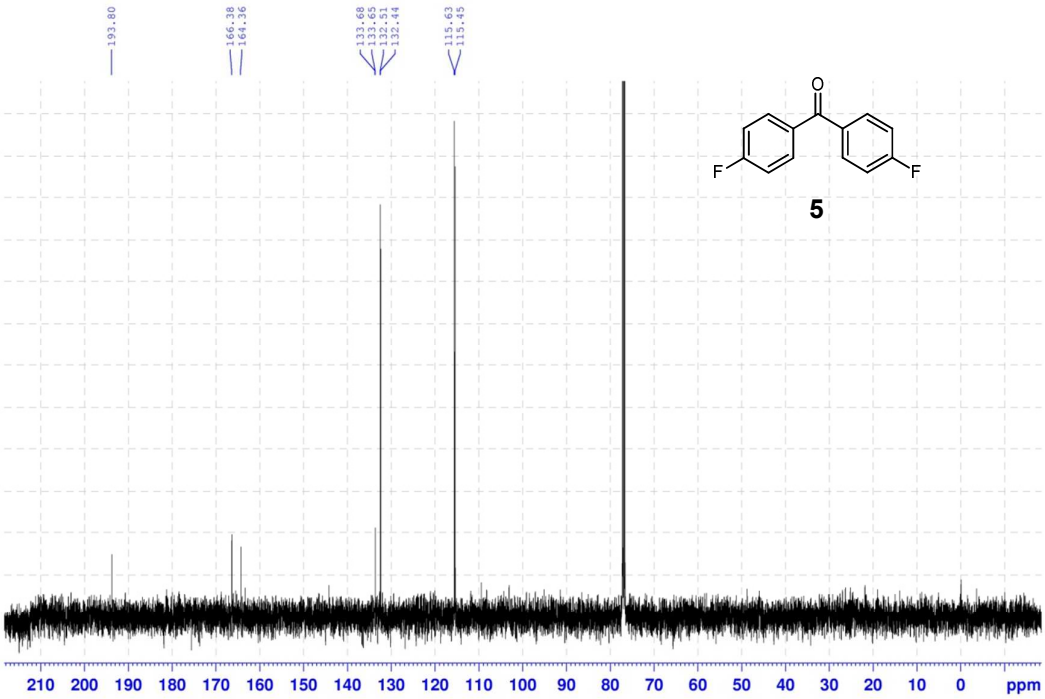
193.80
166.38
164.36
133.68
133.65
132.51
132.44
115.63
115.45
O
F
F
5
210
200
190
180
170
160
150
140
130
120
110
100
90
80
70
60
50
40
30
20
10
0
ppm

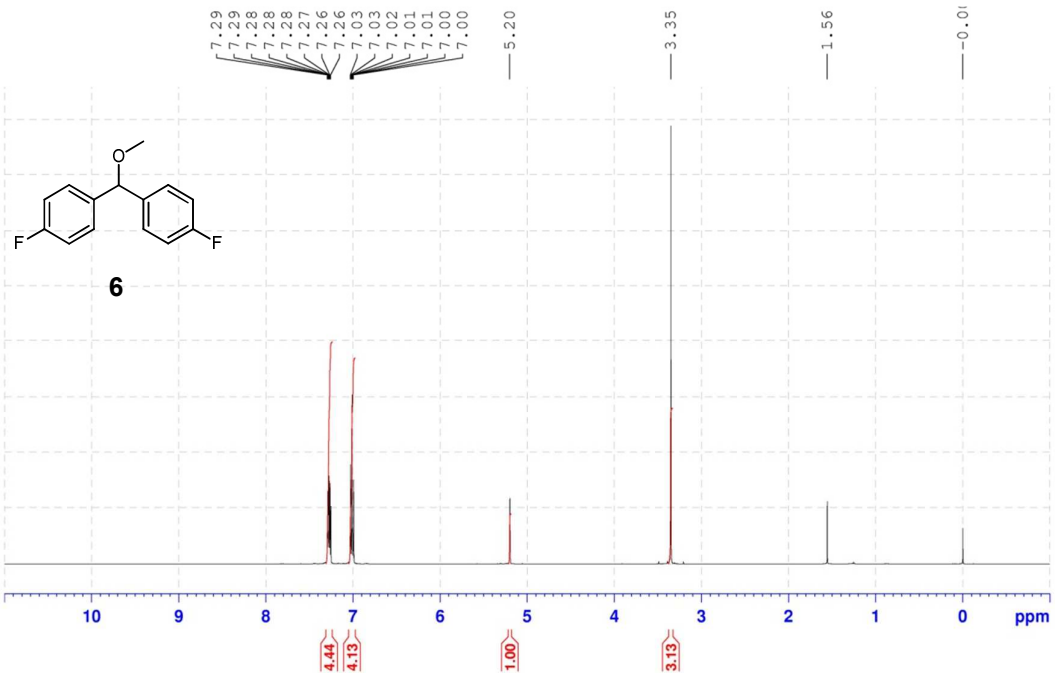
7.29
7.29
7.28
7.28
7.28
7.27
7.26
7.26
7.03
7.03
7.02
7.01
7.01
7.00
7.00
5.20
3.35
1.56
O
F
F
6
10 9 8 7 6 5 4 3 2 1 0 ppm
4.44
4.13
1.00
3.13

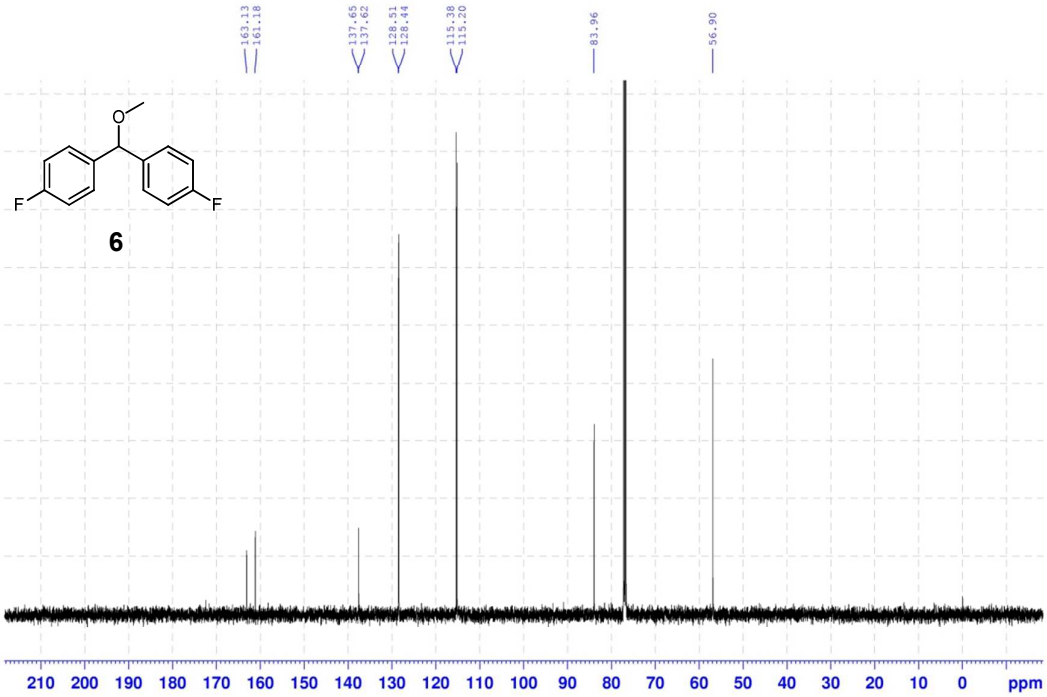
163.13
161.18
137.65
137.62
128.51
128.44
115.38
115.20
83.96
56.90
O
F
F
6
210 200 190 180 170 160 150 140 130 120 110 100 90 80 70 60 50 40 30 20 10 0 ppm